



Recovery of copper from electronic waste: An energy transition approach to decarbonise the industry

Jorge Torrubia ^{a,b}, Ashak Mahmud Parvez ^{a,*}, Mohsin Sajjad ^a, Felipe Alejandro García Paz ^a, Karl Gerald van den Boogaart ^{a,c}

^a Helmholtz-Zentrum Dresden - Rossendorf e.V. (HZDR), Helmholtz Institute Freiberg for Resource Technology (HIF), Chemnitzer Str. 40, 09599, Freiberg, Germany

^b Research Institute for Energy and Resource Efficiency of Aragón (Energaia) - University of Zaragoza, Campus Río Ebro, Mariano Esquillor Gómez, 15, 50018, Zaragoza, Spain

^c Institut für Stochastik, TU Bergakademie Freiberg, Priifer Str. 9, 09596 Freiberg, Germany

ARTICLE INFO

Handling Editor: Panos Seferlis

Keywords:

Copper recovery
Circular economy
Energy transition
WEEE
Waste PCB
Life cycle assessment

ABSTRACT

Copper is essential for a decarbonised economy, yet its production remains heavily dependent on primary extraction processes which still rely on fossil fuels. Thus, there is growing interest in recovering copper from secondary sources, such as waste electrical and electronic equipment (WEEE). Moreover, the potential for utilising renewable resources in copper recycling remains unexplored. Therefore, this study applied FactSage and HSC Chemistry software to model and simulate the pyrometallurgical route for copper recovery from copper scrap and waste printed circuit boards (WPCB). OpenLCA was employed for a life cycle assessment (LCA) of three scenarios: (i) conventional, (ii) green hydrogen, and (iii) hydrogen produced using grid electricity. The results showed that the carbon footprint of copper production was reduced by 71–96% in the conventional scenario (0.3–0.5 kg-CO₂-eq./kg-Cu) and by 93–97% in the green hydrogen scenario (0.1–0.2 kg-CO₂-eq./kg-Cu) compared to primary production. However, the use of hydrogen produced with grid electricity resulted in a significant increase in the carbon footprint, even exceeding the conventional scenario. Therefore, the integration of renewable energy sources is crucial for achieving low-emission secondary copper production, contributing to a cleaner metal supply for the energy transition.

1. Introduction

Electrification is the cornerstone of the energy transition and decarbonisation (Hund et al., 2020). Two key pillars for electrification are renewable energies and electric mobility, which heavily rely on copper. For instance, photovoltaic panels require 3.7–4.6 ton/MW, wind turbines need 1–5 ton/MW (European Commission: Joint Research Centre et al., 2020) and electric vehicles use four times more copper than combustion vehicles (International copper study group). The demand of these technologies will surge due to the efforts of decarbonisation, increasing the demand of copper with them (Hund et al., 2020). To provide context: it is projected that 550 million tons of copper will be extracted in the next 25 years, which is equivalent to the amount of copper that has been mined over the past 5000 years (Hund et al., 2020; Tabelin et al., 2021). The continued extraction of copper resources has caused a decline in the ore grade, since it was around 2.5% in the early 20th century, but by 2015, it had decreased to 0.6% (Dong et al., 2020).

This decline in ore grades is associated to an exponential increase in energy consumption, (mainly from fossil fuels), water consumption and greenhouse gas emissions, which means an exponential increase in environmental damage (Dong et al., 2020; Northey et al., 2014; Van der Voet et al., 2019). Furthermore, low-grade deposits also contain high concentrations of impurities, such as arsenic (As) and antimony (Sb), resulting in impure concentrates that are penalised or even rejected by smelters (Tabelin et al., 2021; Nazari et al., 2017).

Now the paradox becomes evident: a massive amount of copper is required to electrify the economy, but its extraction depends highly on fossil fuels (Torrubia et al., 2023a), and mines are approaching the lower limits of cut-off grades (Mills 2022). In this context, copper recovery from waste offers a partial solution, since mining will still be required to supply metals (Hund et al., 2020). This recovery majorly presents two advantages: (i) it requires lower consumption of fossil fuels and thus lower carbon emissions and (ii) it can reduce primary extraction. This could alleviate the environmental impact on extractive countries (e.g.

* Corresponding author.

E-mail address: a.parvez@hzdr.de (A.M. Parvez).

biodiverse territories in Chile, Peru or Democratic Republic of Congo, which constitute almost 50% of the global production (National Minerals Information Center), and conserve these resources for future generations (Lazard and Youngs, 2021).

From a geopolitical point of view, since March 2023, copper has been included in the European Commission's list of strategic raw materials due to its economic importance in strategic sectors together with difficult substitution, and dependence on third countries supplies (European Commission; Directorate-General for Internal Market; Industry; Entrepreneurship and SMEs et al., 2023). Therefore, it is essential to increase the secondary copper production in European countries. In this respect, WEEE are highly promising secondary source of copper since they were the largest copper-bearing waste globally generated between 1980 and 2010 (Tabelin et al., 2021). Additionally, WEEE generation is increasing by 3–5% annually, three times faster than the municipal solid waste (MSW) (Torrubia et al., 2023b). WEEE contributes up to 70% of hazardous waste in landfills, therefore recycling it can significantly decrease the environmental impact of MSW (Forti et al., 2018). Europe leads in WEEE generation per capita (Forti et al., 2018). The ProSUM Project (Huisman et al., 2017) reported that between 2000 and 2020, the European market consumed 760,000 tons of brass, 450,000 tons of bronze and 4,500,000 tons of other copper alloys, and 4,400,000 tons of printed circuit boards (PCB), considering only electric and electronic equipment (EEE). These quantities, with high copper content alloys (60–90%) and PCB (5–65%) (Torrubia et al., 2022), will be available for recovery in a few years as EEE usually reaches their end-of-life between 2 and 10 years (Forti et al., 2018).

Waste PCB (WPCB) are the most complex fraction of WEEE. Although WPCB generates hazardous gases when their plastics are burnt, they replace coke as a reducing agent (Khaliq et al., 2014; Valero Navazo et al., 2014). However, treating these off-gases is expensive, as exemplified by Umicore's investment of over 200 million € to upgrade their plant for this purpose (Valero Navazo et al., 2014). The pyrometallurgical route has been considered as the preferred method for copper recovery from WPCB and copper-rich scrap due to its cost-effectiveness and eco-efficiency (Khaliq et al., 2014). Therefore, this technology enables large companies, such as Boliden (Ronskar, Sweden), Umicore (Antwerp, Belgium), Aurubis (Lünen, Germany) and Brixlegg (Austria), Xstrata (Canada), and Dowa (Japan) to achieve recovery rates of over 90% (Valero Navazo et al., 2014). However, it requires advanced technology for process optimisation with high capital investments and operating costs (Tabelin et al., 2021; Khaliq et al., 2014; Valero Navazo et al., 2014).

Many researchers have investigated copper recovery from waste by using different approaches (Dong et al., 2020; Ghodrat et al., 2018, 2019; Hong et al., 2018; Chen et al., 2019; Zhang et al., 2021, 2022; Mairizal et al., 2023a). Few studies were focused on the thermodynamics and distribution of the elements in the pyrometallurgical route, such as Shuva et al. (2016) or Chen et al. (2021). Others used software, like FactSage or HSC Chemistry, to simulate this route, such as Ghodrat et al. (2018). However, these studies did not explore LCA of the process. On the other hand, LCA of secondary copper was also studied by many researchers (Hong et al., 2018; Chen et al., 2019; Zhang et al., 2021, 2022; Mairizal et al., 2023a; Dong et al., 2022). For example, Ghodrat et al. (2017) performed a LCA, but without further discussion on the implications of the energy transition. Other studies, like Dong et al. (2020) or Mairizal et al., 2023a, 2023b, focused on the LCA and energy transition, but without considering the use of renewable fuels (such as green hydrogen) in all stages of recycling. Finally, Röben et al. (2021) focused on energy transition by establishing scenarios using green hydrogen, but secondary copper production was not considered. Therefore, to the best of author's knowledge, this is the first study that combines simulation-based data with different decarbonisation scenarios using green hydrogen and LCA evaluation methodology to better understand the potential for decarbonisation of the secondary copper production.

This paper first presents the methodology, outlining all simulation cases conducted using FactSage and HSC software (sections 2.1 and 2.2). Further details on the simulations are provided in the Supplementary Information (SI). Section 2.3 describes the LCA methodology. In results section, simulation outcomes are first compared with reported works (in section 3.1), followed by the LCA results in section 3.2. The conclusion section summarises the key finding of this study.

2. Data and methodology

2.1. WEEE composition and the three simulation cases

This study considered two specific type of copper-rich wastes (Scrap and WPCB) which assumed to be the representative of WEEE. Their characteristics are provided as below.

- **Scrap:** scrap contains around 75 wt% Cu, reflecting the copper content of alloys, which ranges 60–90 wt%-Cu. Table 1 shows the composition, which was estimated based on alloy scrap from the Institute of Scrap Recycling Industries (ISRI). Approximately 5 wt% consists of oxides, in the form of Cu₂O.
- **WPCB:** WPCB typically contain around 5–65 wt% Cu and constitute the most complex and variable waste among WEEE (Torrubia et al., 2022; Khaliq et al., 2014). This variability in composition affect the results since WPCB contain a considerable amount of precious metals (such as Au and Ag) and critical metals (such as Pd, Ta or Co) with high price. Table 2 summarises the composition of WPCB considered in this study.

This study investigates three cases to cover different waste compositions, given the significant variation in copper content, particularly in WPCB.

- **Scrap case:** input is 20 ton/h of scrap.
- **Mix case:** input is 10 ton/h of scrap and 10 ton/h of WPCB.
- **WPCB case:** input is 20 ton/h of WPCB.

2.2. FactSage and HSC Chemistry simulations

Fig. 1(a) shows the Block Flow Diagram (BFD) for the copper recovery from the three cases mentioned in the previous section (Scrap, Mix and WPCB) and Fig. 1(b) depicts the simulation flowsheet developed in HSC Chemistry (Outotec Research Center HSC Chemistry 10). This figure shows all the flows, including the recirculation of slag and anode, a practice common in the copper industry (Khaliq et al., 2014; Valero Navazo et al., 2014; Schlesinger et al., 2021), but frequently missing in reported simulation-based studies (Ghodrat et al., 2017, 2018, 2019; Mairizal et al., 2023a, 2023b). The most important units are: (1) shredding, (2) reduction, (3) oxidation, (4) heat recovery, (5) fire refining, (6) electrorefining, (7) air separation unit (ASU), and (8) electrolyzers.

FactSage was used to calculate the composition of the flows in the pyrometallurgical processes: (2) reduction, (3) oxidation, and (5) fire refining. Table 3 shows the operational parameters (*i.e.* temperature, partial pressure of oxygen (ppO₂)), inputs, and outputs of all the pyrometallurgical processes compared to literatures. These parameters were adopted from thermodynamic (Shuva et al., 2016; Chen et al., 2021; Ghodrat et al., 2017), industrial (Schlesinger et al., 2021), and

Table 1
Scrap composition (Institute of Scrap Recycling Industries).

Scrap (wt%)	Cu	Cu ₂ O	Sn	Pb	Zn	Ni
Total Metallic	73	3.5	3	5	15	0.5
100%						

Table 2
WPCB composition (Torrubia et al., 2022; Khaliq et al., 2014).

WPCB (wt%)	Cu	Fe	Al	Sn	Pb	Ni	Zn	Ag	Au	Pd	Ta	Co
Total Metallic	Cu	Fe	Al	Sn	Pb	Ni	Zn	Ag	Au	Pd	Ta	Co
40	22	6	4	3	3	1	0.8	0.1	0.04	0.02	0.02	0.02
Total Plastic	C ₆ H ₆	C ₂ F ₄	C ₂ H ₆		C ₂ H ₃ Cl		C ₁₀ H ₂₀ O ₂		C ₁₅ H ₁₆ O ₂		C ₁₂ H ₂₂ O ₄	
30	5	2	10		2		5		5		1	
Total Ceramic	SiO ₂	MgO	Al ₂ O ₃		CaO		K ₂ O		Na ₂ O		TiO ₂	
30	15	2	6		1		1		2		3	

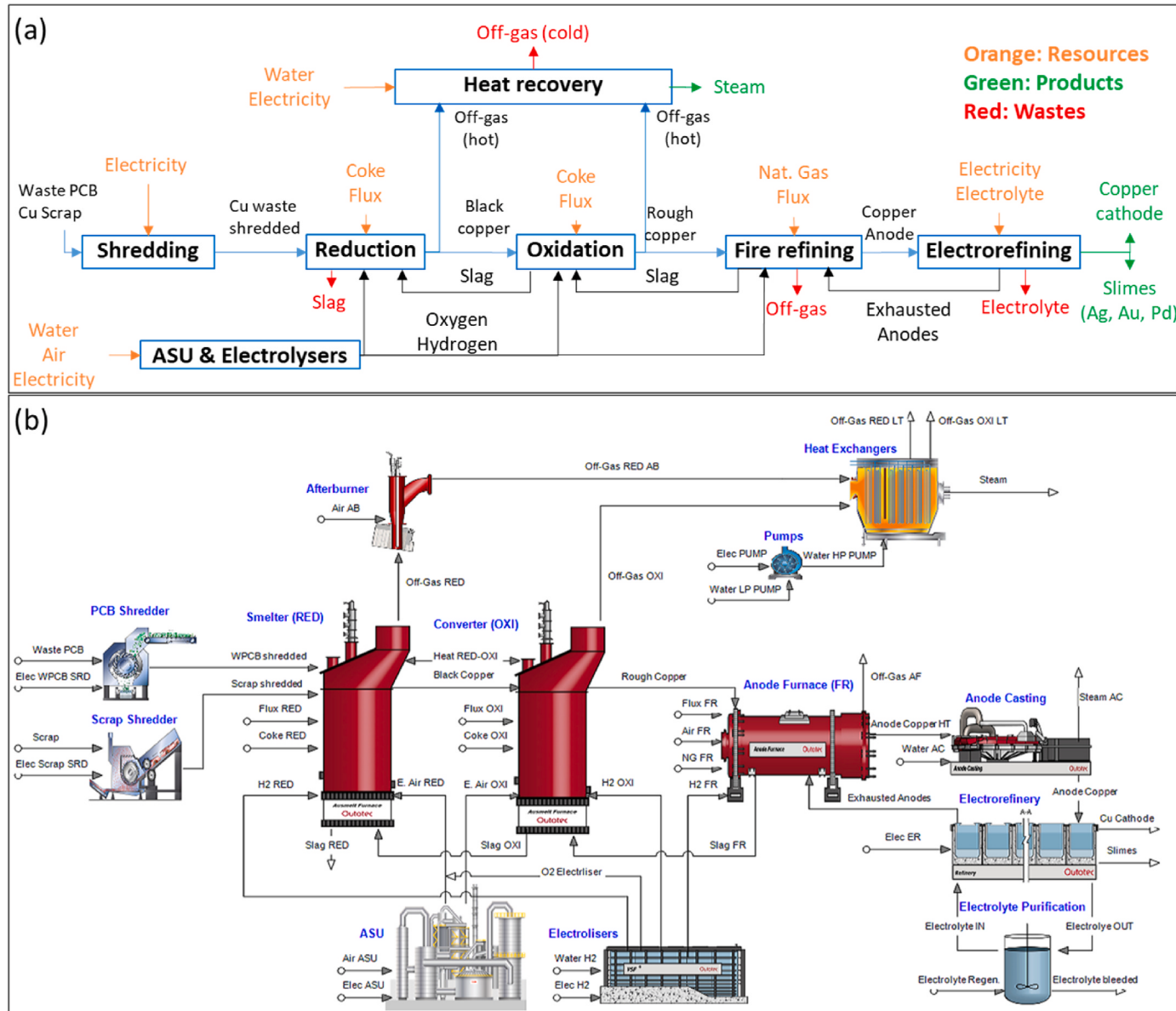


Fig. 1. (a) Block flow diagram of the copper recovery process and (b) HSC Chemistry simulation flowsheet of copper recovery process.

experimental data (Chen et al., 2021; Felkl et al., 2023; Anindya, 2012) in the studied simulation. The complete calculation procedure and the deviation of few results compared to literatures are explained in section S1 of SI. These deviations occur due to the recirculation of slag and anode and processing of different feed in this study. For instance, this study uses higher WPCB percentages (50–100%) in the feed compared to the literatures (10–30%) (Ghodrat et al., 2019; Mairizal et al., 2023b) due to the expected increase of WPCB in copper-rich waste because of

the digital transition (Forti et al., 2018; Huisman et al., 2017).

HSC simulation was performed using FactSage results derived from pyrometallurgical units and also used to model the other units (see section S2 of SI) and characterising all the flows. Depending on the energy source used, two type of simulations were conducted.

Table 3

Input, output, and operational parameters of the pyrometallurgical units used in FactSage simulation.

Unit	Reduction						Oxidation						Fire Refining									
	Literature		This study (conv.)		This study (Hydrogen)		Literature		This study (conv.)		This study (Hydrogen)		Literature		This study (conv.)		This study (Hydrogen)					
	Scrap	Mix	WPCB	Scrap	Mix	WPCB	(Ghodrat et al., 2019; Shuva et al., 2016; Chen et al., 2021; Ghodrat et al., 2017; Schlesinger et al., 2021; Felkl et al., 2023; Anindya, 2012)	Scrap	Mix	WPCB	Scrap	Mix	WPCB	(Ghodrat et al., 2019; Shuva et al., 2016; Chen et al., 2021; Ghodrat et al., 2017; Schlesinger et al., 2021; Felkl et al., 2023; Anindya, 2012)	Scrap	Mix	WPCB	Scrap	Mix	WPCB		
Operational parameters																						
Temperature	°C	1200–1400	atm	10 ⁻⁷ –10 ⁻⁹	1300	1300	1300	1300	1300	1300	1200–1400	1300	1300	1300	1300	1300	1200–1300	1300	1300	1300		
ppO ₂					10 ⁻⁹	10 ⁻⁹	10 ⁻⁹	10 ⁻⁹	10 ⁻⁹	10 ⁻⁹	10 ⁻⁵ –10 ⁻⁶	10 ⁻⁶	10 ⁻⁶	10 ⁻⁶	10 ⁻⁶	10 ⁻⁶	10 ⁻⁶ –10 ⁻⁷	10 ⁻⁶	10 ⁻⁶	10 ⁻⁶		
Input																						
Air	t/h	0.07	16	35	0.01	16	34					2.95	2.5	2.5	3.15	2.5	3.0		8.24	5.2	6.3	
Coke/H ₂ /NG	t/h	0.22	0	0	0.095	0	0					0.2	0.2	0.23	0.04	0.14	0.11		0.38	0.24	0.31	
Flux	t/h	0	0	4.54	0	0	9					8.61	7.0	4.9	9.11	7.0	4.2		4.98	3.13	1.31	
Output																						
Black Copper										Rough Copper												
Cu	wt. %	74–85	78.3	81.4	75.5	80.2	79.7	75.6	95–97	96.5	96.4	96.3	96.9	95.3	96.1	>98	98.3	97.6	98.0	98.4	98.1	97.6
Sn	wt. %	6–8	9.8	10.6	16.1	8.2	11.7	15.6	–	1.19	1.82	1.78	1.23	1.55	1.84	–	1.03	0.87	0.41	0.88	0.36	0.62
Pb	wt. %	5–6	5.9	3.4	1.2	6.2	3.0	1.3	–	1.49	0.04	0.04	1.11	0.85	0.04	–	0.06	0.00	0.09	0.14	0.05	0.00
Zn	wt. %	1–3	1.7	1.2	0.03	1.2	1.6	0.04	–	0.00	0.00	0.00	0.00	0.01	0.00	–	0.00	0.00	0.00	0.00	0.00	0.00
Ni	wt. %	1–3	1.0	2.2	5.5	1.2	2.0	5.6	–	0.64	1.46	1.09	0.53	1.00	1.19	–	0.48	1.13	0.73	0.53	0.30	0.92
Fe	wt. %	5–8	3.2	1.1	1.2	2.9	1.9	1.4	–	0.18	0.17	0.11	0.13	0.11	0.12	–	0.17	0.21	0.10	0.06	1.06	0.06
O	wt. %	–							–							<0.3	0.27	0.3	0.28	0.27	0.2	0.14
Slag																						
Cu ₂ O	wt. %	0.6–1	0.7	0.97	0.7	0.7	0.94	0.8	10–30	11.3	16.8	22.0	17.5	12.1	20.6	–	13.83	12.02	20.17	16.37	15.49	10.88
SnO	wt. %	0.5–0.8	2.3	0.97	0.9	2.7	2.7	1.2	5–15	10.7	10.5	13.5	8.7	11.2	13.1	–	0.68	3.05	4.01	1.24	2.72	3.25
PbO	wt. %	–	3.90	0.01	0.01	3.80	0.01	0.01	5–15	5.1	3.4	1.0	5.8	1.3	1.0	–	1.97	0.05	0.03	0.95	0.35	0.03
ZnO	wt. %	3.5–4.5	19.0	4.3	0.7	18.7	6.4	0.5	3–6	2.1	1.4	0.03	1.5	1.6	0.04	–	0.00	0.00	0.00	0.00	0.02	0.00
NiO	wt. %	–	0.18	0.29	1.04	0.12	0.87	0.82	1–5	0.9	1.7	5.5	1.1	2.0	5.2	–	0.64	1.34	1.44	0.13	1.84	0.98
Off-gas																						
CO ₂	t/h	–	0.61	7.18	15.3	0	6.84	14.8	–	0.64	0.65	0.75	0	0	0	–	1.02	0.64	0.84	0	0	0
CO	t/h	–	0.26	0.46	0.35	0	0.97	0.90	–	0.01	0.01	0.01	0	0	0	–	0.01	0.01	0.01	0	0	0
HF	t/h	–	0	0.16	0.32	0	0.17	0.33	–	0	0	0	0	0	0	–	0	0	0	0	0	0
HCl	t/h	–	0	0.12	0.23	0	0.12	0.24	–	0	0	0	0	0	0	–	0	0	0	0	0	0

- **Conventional simulation:** This simulation utilised conventional fuels: coke for reduction and oxidation, and natural gas for fire refining.
- **Hydrogen simulation:** This simulation used hydrogen (H_2) for the reduction, oxidation and fire refining. Although hydrogen is not yet adopted in the copper industry, its viability has been demonstrated in various applications such as burners, anode refining furnaces and melting units (Röben et al., 2021). Hydrogen has also been successfully utilised as a copper reductant (Qu et al., 2020) and in industrial furnaces by large companies (Torben and Steindor, 2023). Furthermore, recent projects show the growing interest in hydrogen (Hydrogen As the Reducing Agent). The hydrogen was produced in an electrolyser using electricity. Furthermore, part of required oxygen was generated as by-product, which reduce the need for oxygen production in the ASU.

2.2.1. Shredding

The shredding step reduced the size of waste (Scrap, Mix or WPCB) in the range of 10–20 mm for feeding into the smelter (RED). In this step, electricity was consumed in the shredding machine. Since the scrap and WPCB have different physical properties, the energy consumption varied depending on them. Industrial data from Taiwanese factories (Pokhrel et al., 2020) was assumed for WPCB (44 kWh/ton-WPCB), whereas for scrap, machinery consumption was estimated from industrial catalogues (Sicon EcoShred Catalog) (49.6 kWh/ton-scrap). This step was modelled with HSC Chemistry and the electricity consumption for each case is available in section S2.1 of SI.

2.2.2. Reduction

This study used the "reverse Knudsen" configuration, in which the reduction is the first step, and the oxidation is the second. This configuration is used when the feed is oxidised and requires a reduction step to produce metallic copper (Anindya, 2012). It was considered that the reduction and the oxidation processes occurred together in a TSL furnace (Ghodrat et al., 2017), although they were simulated separately. Coke was used in the conventional simulation and hydrogen in the hydrogen simulation.

The distribution of the elements of the different flows was obtained through FactSage (Bale et al., 2016) using the "Equilib" module. This module incorporates the Gibbs free energy minimisation technique to predict the equilibrium of multicomponent and multiphase systems at various processing conditions. Fig. 1 shows that reduction had five inputs: (1) waste, (2) flux, (3) enriched air, (4) coke/hydrogen, and (5) slag recirculated from oxidation; and three outputs: (1) black copper, (2) slag, and (3) off-gases. First, only WPCB or scrap was the only known input and the control parameters (enriched air, flux, and coke or hydrogen) were modified to maximise the copper recovery and fulfil the other output requirements (e.g. copper content in black copper) based on the literatures (Table 3). Furthermore, the recirculation of the slag from oxidation needed several iterations of the simulations. The SI (S1.1.1, S1.2.1, S1.3.1.) provides additional information on how the simulations were conducted for each case.

2.2.3. Oxidation

The fuels in oxidation were the same as in the reduction: coke for the conventional simulation and hydrogen for the hydrogen simulation. The distribution of the elements was calculated using FactSage following a similar procedure than in the reduction. However, in this case, the priority was to avoid the solids formation in the slags, which hinders the operational performance of the furnace (Schlesinger et al., 2021). The most likely solid formation was in the form of SnO_2 , with high melting point (1630 °C) (Outotec Research Center HSC Chemistry 10). Thus, coke/ H_2 , flux, and enriched air were modified to reach a rough copper (the main product of oxidation) with 95–97 wt% Cu along with a composition of slag and off-gases shown in Table 3. However, some

obtained values were different, especially for Mix and WPCB cases since the feed compositions differs greatly from the literatures, mostly based in Scrap cases. The SI (S1.1.2., S1.2.2., S1.3.2.) contains further information about the simulations.

2.2.4. Heat recovery

Reduction and oxidation steps produced a large amount of hot gases (1300 °C) that were harnessed through heat exchangers. The reduction furnace used an afterburner where air was injected to react with the remaining CO or H_2 to generate more heat. After this, the temperature of the gases reaches 1340–1650 °C. The hot gases from the afterburner and the oxidation furnace then passed through heat exchangers where high-pressure water absorbed the heat to produce high-pressure steam (180 bar and 600 °C) (Zhang et al., 2021). Table S49 (SI section S2.2) shows the water and electricity consumption of the pumps. Once the gases are cooled down, these are usually sent to a scrubber for cleaning since they contain environmentally hazardous substances such as dioxins and furans (Khaliq et al., 2014). However, this cleaning step was not considered in the present study due to the complexity of the simulation which mostly originated from lack of process know-how and relevant data. If considered, both energy consumption and carbon footprint would increase due to the resources used and emissions generated at this stage.

2.2.5. Fire refining

Fire refining took place in an anode furnace. This step removed oxygen from the rough copper by injection of fuel. Natural gas was used in conventional simulation, and hydrogen in hydrogen simulation. FactSage was used to calculate the distribution of the elements. Firstly, fuel (natural gas or hydrogen) was adjusted to fulfil the requirement of 1100 MJ/ton-Cu, reported by copper industry (Schlesinger et al., 2021). Second, the flux quantity was fixed at 30 wt% of rough copper mass (Schlesinger et al., 2021). Finally, the air feed was regulated to achieve the allowable range of the parameters of Table 3 (Cu >98% and O <3% in the anode copper). The SI (S1.1.3., S1.2.3., S1.3.3.) contains further information.

2.2.6. Electrorefining

The final product of fire refining was copper anode at 1300 °C, which was cooled to 25 °C by a water flow, through the anode casting process. After this step, the cooled copper anodes were sent to an electrolytic cell, for the electrorefining (Ghodrat et al., 2017). Here, an electrical potential was applied between a copper anode and a metal cathode in the presence of an electrolyte containing $CuSO_4$ and H_2SO_4 to obtain high-purity cathode copper (99.99%). It was assumed that 15% of the anodes were not electrorefined and were recirculated to the anode furnace, this aligns with typical copper industry data (12–20%) (Schlesinger et al., 2021).

The distribution of the elements was simulated in HSC Chemistry using data from the copper industry (Schlesinger et al., 2021). Detailed information on this distribution is available in Table S50 (SI). Table S51 shows the main operational parameters (Schlesinger et al., 2021). Furthermore, the amount of electrolyte used was 0.56 kg electrolyte/kg copper anode (Ghodrat et al., 2017), and the concentration of H_2SO_4 in the electrolyte was set at 165 g/l. The electrolyte recirculation was set at 0.15 m³ of electrolyte per ton of cathode (Schlesinger et al., 2021). More detailed information is available in the SI (S2.3).

2.2.7. Air separation unit (ASU)

ASU was used for production of enriched air for reduction and oxidation steps. This unit takes the atmospheric air (21% O_2) and produce O_2 . The ASU unit was simulated in HSC Chemistry, considering an energy consumption of 670 MJ per ton of oxygen at 50% O_2 purity, based on an industry scale oxygen separation plant (Banaszkiewicz and Chorowski, 2018).

2.2.8. Electrolyser

Electrolyser was only used in the hydrogen simulation. PEM electrolyser was considered due to the high quality of hydrogen production, high efficiency, low operating temperatures, and flexibility for industrial purposes (Shiva Kumar and Himabindu, 2019). This unit was simulated in HSC Chemistry, considering a 70% of energy efficiency based on industrial data (Shiva Kumar and Himabindu, 2019). The electrolyser also produced O₂ as a by-product, which was utilised in the oxidation step, subsequently decreasing the production of oxygen in the ASU for the hydrogen simulation.

2.3. LCA simulation

The goal of the LCA was to evaluate the environmental impacts of the copper recovery, which comprises three cases (Scrap, Mix and WPCB) and two simulations (conventional and hydrogen). Moreover, the present study considered three scenarios which are as follows: (i) conventional, (ii) green hydrogen, and (iii) hydrogen produced using grid electricity (a.). The purpose of the aforementioned third scenario was to assess the impact of electricity mix on hydrogen production. Fig. 2 illustrates the system boundaries, which include all the inputs (resources required for recycling processes: three cases x three scenarios = nine combinations) and outputs (emissions and products from the recycling processes). Therefore, alloy or PCB production leading to scrap or WPCB was excluded, as they are considered recycling wastes. The functional unit was 1 kg of copper.

The life cycle inventory (LCI) was obtained from the FactSage and HSC simulations, explained in the previous subsection. Tables in section S4 of SI shows the inputs and outputs of all processes and the Ecoinvent providers used for each scenario to link the LCI in OpenLCA.

As shown in Fig. 2, the processes generated three products

simultaneously: copper (reference product), steam (from heat recovery), and slimes (from electrorefining), which contains significant amounts of Au, Ag, and Pd. Therefore, it was essential to allocate the environmental impact associated with each co-product. For this purpose, economic allocation was chosen since it is the most widespread in the case of metals (Dong et al., 2020; Sanjuan-Delmás et al., 2022). Table S4 of SI shows the prices used for this allocation, calculated using the last 10-years average, obtained from (Trading economics Price of Metals). Life cycle impact assessment (LCIA) results were calculated using the CML - IA baseline method, as it is commonly employed for the assessment of metal production (Dong et al., 2020; Van der Voet et al., 2019; Chen et al., 2019; Sanjuan-Delmás et al., 2022). Nine categories were analysed: Abiotic Depletion (AD), Abiotic Depletion - Fossil Fuels (ADff), Acidification (Aci), Eutrophication (EU), Fresh Water Aquatic Ecotoxicity (WT), Global Warming Potential or carbon footprint (GW), Human Toxicity (HT), Marine Aquatic Ecotoxicity (MT), Ozone Layer Depletion (OLD), Photochemical Oxidation (PO), and Terrestrial Ecotoxicity (TT).

3. Results and discussion

3.1. FactSage and HSC Chemistry results

3.1.1. Copper recovery

Table 4 shows the main HSC results derived from the six simulations, compared with findings from the literatures. The results are divided into three main categories: (i) copper recovery; (ii) energy requirements, and (iii) CO₂ emissions. Furthermore, Energy requirements are divided into five steps of the copper recovery process (Fig. 2): (i) shredding; (ii) reduction; (iii) oxidation; (iv) fire refining, and (v) electrolysis. In addition, the oxygen consumption is also indicated in both reduction and oxidation processes. The rest of the results are detailed in the SI

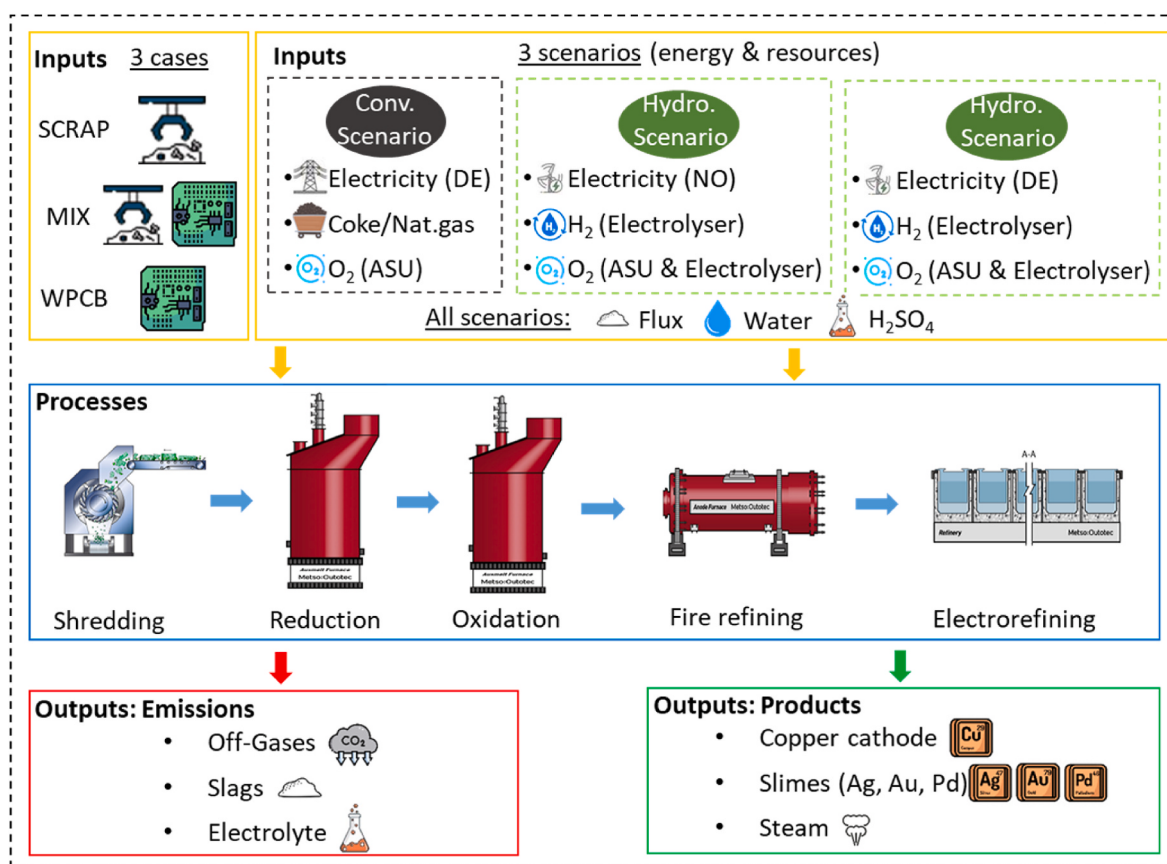


Fig. 2. LCA system boundaries (orange box: inputs; blue box: process steps; red box: emissions and green box: products). (For interpretation of the references to colour in this figure legend, the reader is referred to the Web version of this article.)

Table 4

HSC simulation results (t: ton of copper recovered (ton-Cu)).

Results per ton of copper recovered		Copper	Shred.	Reduction		Oxidation		F. Ref.	E. Ref.	Emissions
		Recovery	Elect.	Coke/ H ₂	O ₂	Coke/H ₂	O ₂	N.Gas/ H ₂	Electr.	CO ₂ -eq.
		%	kWh/ t	GJ/t	ton/ t	GJ/t	ton/ t	GJ/t	kWh/t	ton/t
Scrap	Conv. Sim.[TS]	97.3%	67	0.41	0.0	0.37	0.2	1.2	341	0.16
	Hydr. Sim.[TS]	97.2%	67	0.78	0.0	0.33	0.2	1.0	341	0.00
	Conv. Sim. (Dong et al., 2020; Hong et al., 2018; Chen et al., 2019; Zhang et al., 2021, 2022; Mairizal et al., 2023b)	–	–	^a	–	2.6–18 ^a	–	2.23	286–867	0.3–1.6
	Hydr. Sim. (Mairizal et al., 2023b)	–	–	^a	–	(6.6) ^a	(8.2)	(451)	(0.7)	0.0
Mix (%) WPCB	Conv. Sim.(50%)[TS]	96.7%	99	0	1.7	0.58	0.3	1.2	341	0.97
	Hydr. Sim.(50%)[TS]	96.5%	99	0	1.7	1.8	0.3	1.8	342	0.83
	Conv. Sim.(10–30%) (Ghodrat et al., 2019; Mairizal et al., 2023b)	79–83%	–	^a	–	1.3–9.7 ^a	–	5.8–7.5	–	0.2–4.8
	Hydr. Sim.(10%) (Mairizal et al., 2023b)	–	–	0	–	1.3	–	–	–	0.0
WPCB	Conv. Sim. [TS]	94.9%	210	0	8.3	1.5	0.6	3.6	341	4.17
	Hydr. Sim. [TS]	94.1%	212	0	8.2	3.2	0.7	2.9	341	3.82
	Conv. Sim. (Valero Navazo et al., 2014; Fujita et al., 2014)	–	297	^a	–	3.7–3.9 ^a	–	7.5	349	–

^a also includes reduction process. Parentheses show the average values. Conv. Sim.: Conventional Simulation; Hydr. Sim.: Hydrogen Simulation, TS: This study.

(section S2).

Copper recovery ranged from 94 to 95% in the WPCB case to over 97% in the Scrap case. This difference is attributed to the different copper concentrations in the feed since copper was more concentrated in the scrap, (approximately 75%), and therefore easier to recover, compared to WPCB (approximately 20%). These recovery rates surpassed those reported in the literatures (ranging between 78.8% and 83.3%), as those studies did not consider the recirculation of the slags (*i.e.* fire refining slag to the oxidation, and oxidation slag to the reduction processes) and the exhausted anodes from electrorefining. The oxidation and fire refining slags contain 11.3–21.9 wt%-Cu₂O (see SI section S1) and 15 wt% of the anodes (97.6–98.4 wt%-Cu) in electrorefining remains non-electrorefined. Therefore, without recirculation, this copper would be directly lost. Consequently, oxidation is the less efficient step, resulting in a loss of 11.9–32.1 wt%-Cu, followed by electrorefining (14.8 wt%-Cu), fire refining (3.5–6.4 wt%-Cu) and reduction (0.66–2.8 wt% Cu). However, overall copper losses were minimised until 2.7–5.9 wt%-Cu through recirculation. Further details on copper losses are available in SI (section S3). Additionally, the higher copper recovery rate in this study compared to the literatures further elucidates the lower energy consumption and CO₂ emissions per ton of copper recovered, as outlined in the following subsections.

3.1.2. Energy consumption

The shredding step showed a lower electricity consumption per ton recovered (67 kWh/ton-Cu) in the Scrap case compared to the Mix (99 kWh/ton-Cu) and the WPCB case (210 kWh/ton-Cu), attributed to energy normalisation per ton of copper recovered since more copper is recovered in the Scrap case (14.8 tons) compared to the others (*i.e.* 9.5 and 4.1 tons). Moreover, electricity consumption in the WPCB case (210 kWh/ton-Cu) aligned with the literature results (297 kWh/ton-Cu (Valero Navazo et al., 2014)). This minor difference can be attributed to the selection of different shredding equipment.

The reduction step in the Mix and WPCB cases did not consume coke since plastics embedded in the WPCB were sufficient to carry out the reduction and provide the energy for the process. A study conducted in Umicore (Valero Navazo et al., 2014), showed no differences in recovery rates or operating stability when running with plastics embodied in electronic waste. WPCB and Mix cases required more enriched air (8.3 and 1.7 tons/ton-Cu) compared to Scrap case (0.01 tons/ton-Cu) due to the need of burning the plastics. The oxidation step demanded higher

fuel and oxygen consumption in WPCB cases (1.5–3.2 GJ/ton-Cu and 0.6–0.7 tons-O₂/ton-Cu) compared to Mix (0.6–1.8 GJ/ton-Cu and 0.3 tons-O₂/ton-Cu) or Scrap (0.3–0.4 GJ/ton-Cu and 0.2 tons-O₂/ton-Cu). This is attributed to the higher oxygen requirement to oxidise the impurities in the MIX and WPCB cases, since WPCB contains higher concentrations of impurities (only 20% of copper). The energy consumption of the reduction and oxidation steps (0.6–3.2 GJ/ton-Cu) was lower compared to literature values in Table 4 (1.3–9.7 GJ/ton-Cu, with an average around 6.6 GJ/ton-Cu), attributable to the higher copper recovery in this study. However, Table 4 shows the considerable variability of the results reviewed in the literatures. For instance, results from Zhang et al. (2021) (reaching up to 18.5 GJ/ton-Cu) differed significantly but is attributed to the lower copper content and higher humidity of the feed.

The natural gas and hydrogen consumption in the fire refining ranged from 1.0 to 3.6 GJ/ton-Cu showing an increasing trend for the Mix and WPCB cases in relation to Scrap case. This effect is produced owing to the presence of more oxygen in rough copper in Mix and WPCB cases, which must be removed in this step. These results were consistent with other studies, which ranged from 2 to 23 GJ/ton-Cu (8.2 GJ/ton-Cu in average). Again, the lower values achieved in this study can be attributed to the higher recovery rates. The literatures also shows a significant variability at this stage. For instance, the results reported by Chen et al. (2019) and Dong et al. (2022) were nearly one order of magnitude higher (ranging from 18 to 23 GJ/ton-Cu). These differences can be associated with the use of natural gas in other processes apart from fire refining.

Electricity consumption in electrolysis remains constant in all cases (341–342 kWh/ton-Cu), as identical parameters were employed for all cases and simulations. These values fall within the range observed in previous studies (286–867 kWh/ton-Cu (451 kWh/ton-Cu average)).

3.1.3. CO₂ emissions and the combustion of plastics of WPCB

The Scrap case showed lower CO₂ emissions (0.16 ton-CO₂-eq./ton-Cu) than literature values (0.3–1.6 ton-CO₂-eq./ton-Cu) due to the lower energy consumption per ton of recovered copper caused by the higher recovery rate, as discussed previously. However, the Mix case (0.8–1.0 ton-CO₂-eq./ton-Cu) shows values in range with the literatures (0.2–4.8 ton-CO₂-eq./ton-Cu) as in this case the role of plastics become more important than energy consumption regarding CO₂ emissions.

In order to understand the role of plastics in Mix and WPCB cases

with regard to CO₂ emissions, Fig. 3 illustrate the relationship between CO₂ emissions and energy consumption for the three cases. It demonstrates that higher the proportion of WPCB (Mix case = 50% and WPCB case = 100%) the greater the CO₂ emissions relative to the energy consumption. In the Scrap case (76% copper), 3.5 GJ/ton-Cu were required, emitting 0.16 tons-CO₂-eq./ton-Cu, whereas in the WPCB case (22% copper), 10 GJ/ton-Cu emitted 4.17 tons-CO₂-eq./ton-Cu. Thus, while energy requirements increased less than three-fold, emissions increased by 26 times, although WPCB plastics replaced the consumption of coke or hydrogen during reduction step. Therefore, it is deduced that the energy contained in WPCB plastics is higher than energy required for the reduction process. Consequently, the industry could separate the plastics previously for recycling. This strategy present two advantages: (1) recycled plastics would serve as an additional product and (2) avoidance of CO₂ emissions and other gases from plastics would reduce cost associated with gas treatment (Valero Navazo et al., 2014).

3.2. LCA simulation results

3.2.1. The effect of economic allocation

Economic allocation is critical to understand the LCA results. Fig. 4 shows that copper only contributes 17.7–21.6% in Mix and 4.8–5.1% in WPCB case to the carbon footprint (GW) due to the higher prices of Au, Pd, and Ag. These percentages are constant along all the impact categories. Thus, without considering allocation, WPCB cases would exhibit higher environmental impacts in the categories AD, ADff, Aci, EU, GW, OLD, and PO, followed by Mix and Scrap. However, when considering economic allocation (Table 5), the impact order gets reversed, with Scrap cases having the highest impact, followed by Mix and WPCB (these findings are reflected numerically in Fig. 4). This demonstrates the key role of precious metals in determining the environmental impact of copper in the Mix and WPCB cases.

On the other hand, the toxicity categories (WT, HT, MT and TT) demonstrate a different pattern. When no allocation is considered, WT and TT have similar impacts. Hence, considering economic allocation, Scrap cases had the most significant impact, followed by Mix and WPCB. In the HT and MT categories, WPCB and Mix cases showed substantially higher impacts compared to Scrap due to the toxins produced in WPCB combustion. Therefore, when considering allocation in Table 5, the three cases presented a similar impact.

3.2.2. Global warming potential (GW) assessment

Fig. 5 shows the contribution of each step to the GW (global warming potential), considering both direct emissions (legend: RED, OXI and FREF) and indirect emissions (legend: Electricity, H₂SO₄, Fuel, O₂ and

flux). We validated our GW results with those found in the literatures. However, the current studies mainly focus on conventional fuels, limiting the comparisons to this scenario. Regarding scrap, few literatures findings have been reported 0.30 kg-CO₂-eq. (Chen et al., 2019), 0.60 kg-CO₂-eq. (Hong et al., 2018), 1.25 kg-CO₂-eq. (Zhang et al., 2022), and 1.59 kg-CO₂-eq. (Dong et al., 2020), which are consistent with our results (0.54 kg-CO₂-eq./kg-Cu). In the case of WPCB, the reference (Mairizal et al., 2023a) reported 1.9–3.8 kg-CO₂-eq./kg-Cu, which contrasts with our result (0.26 kg-CO₂-eq./kg-Cu). However, this difference is explained by Fig. 4, because the concentration of precious metals in WPCB is critical due to economic allocation of GW, which increase to 5.3 kg-CO₂-eq./kg-WPCB without considering the allocation. Nevertheless, when allocation is considered, secondary production consistently shows a lower GW (0.13–0.89 kg-CO₂-eq./kg-Cu) compared to primary production, including pyrometallurgical (3.5–6 kg-CO₂-eq./kg-Cu) or hydrometallurgical (1.9–7.4 kg-CO₂-eq./kg-Cu) processes (Dong et al., 2020; Van der Voet et al., 2019; Zhang et al., 2022; Sanjuan-Delmás et al., 2022).

First, the results of conventional scenario (CS) and hydrogen scenario (HS) are analysed. Fig. 5 shows that the conventional scenario always represented the most significant emissions: 0.54 kg-CO₂-eq. in the Scrap case, 0.32 kg-CO₂-eq. in the Mix case, and 0.26 kg-CO₂-eq. in the WPCB case (without considering HS-GE scenarios, dashed line). The lower emissions in hydrogen scenario occurred mainly due to the following three reasons: (i) the direct emissions of the oxidation step (legend: OXI) were zero as hydrogen does not produce CO₂ (furthermore, in the Scrap case, the reduction (legend: RED) also had no emissions due to the absence of WPCB); (ii) the fuels needed for oxidation (legend: OXI fuel) had lower indirect emissions in hydrogen scenario, since the production of hydrogen report lower footprint than coke production, and (iii) low-carbon renewable electricity minimised the carbon footprint in electrorefining and shredding processes (legend: EREF Electricity and SRD Electricity). On the other hand, in the conventional scenario, the WPCB and Mix cases present less GW compared to the Scrap case, due to the economic allocation (see Fig. 4). However, in the hydrogen scenario, the trend was reversed, i.e., WPCB and Mix, show higher GW than Scrap. This occurs due to the significant emissions resulting from burning WPCB plastics in the reduction process (RED, represented by the blue bars in Fig. 5), which persist in Mix and WPCB cases in hydrogen scenario. The only way to avoid these emissions would be to separate the plastics before feeding them into the smelter.

Second, the results of hydrogen scenario (HS) and hydrogen scenario with grid electricity (HS-GE) are analysed. HS-GE scenarios exhibited the highest impacts across all cases (0.33, 0.40, and 0.89 kg-CO₂-eq./kg-Cu for WPCB, Mix and Scrap, respectively), surpassing even the conventional scenario (0.26, 0.32, 0.54 kg-CO₂-eq./kg-Cu, respectively). Two factors cause the increase in GW in the HS-GE scenario. First, the hydrogen scenarios are highly electricity-dependent, as hydrogen is obtained from electrolyzers. Second, the GW of electricity in the HS-GE scenario is 33 times higher compared to the HS scenario, due to the higher GW of fossil fuel-based electricity compared to renewable electricity. Thus, this study revealed that recycling copper using hydrogen only becomes reasonable if renewable electricity is used for its production.

Therefore, the green hydrogen scenario is the most favourable, as it achieves a significant carbon footprint reduction (15–76%) compared to conventional cases. However, this decrement is minimal (15%) in the WPCB case due to the burning of plastics. Thus, the industry could benefit from prior recovering the plastics instead of burning, increasing both circularity and reducing emissions. Another key factor is the value of precious metals in WPCB, which can represent 95% of the total value, enhancing the profitability of the process.

The methodology adopted in the present study presents certain limitations, which are the uncertainty of waste feed, limitation of metallurgical modelling and simulations (FactSage and HSC), and the use of hydrogen in copper industry. However, these limitations were

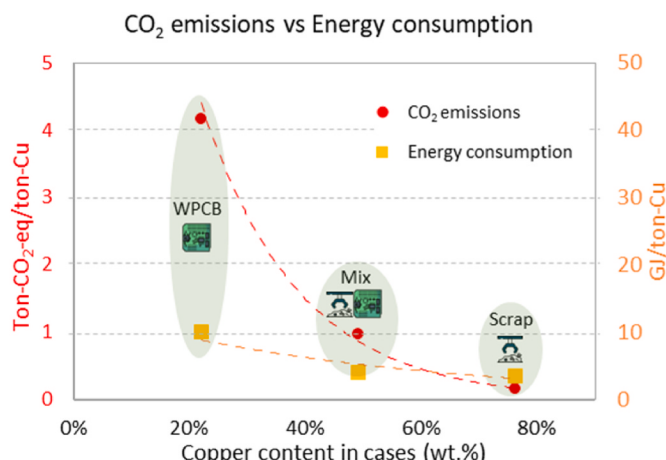


Fig. 3. CO₂ emissions compared to energy consumption (WPCB case 20 wt% Cu, Mix case 50 wt% Cu, Scrap case 75 wt% Cu).

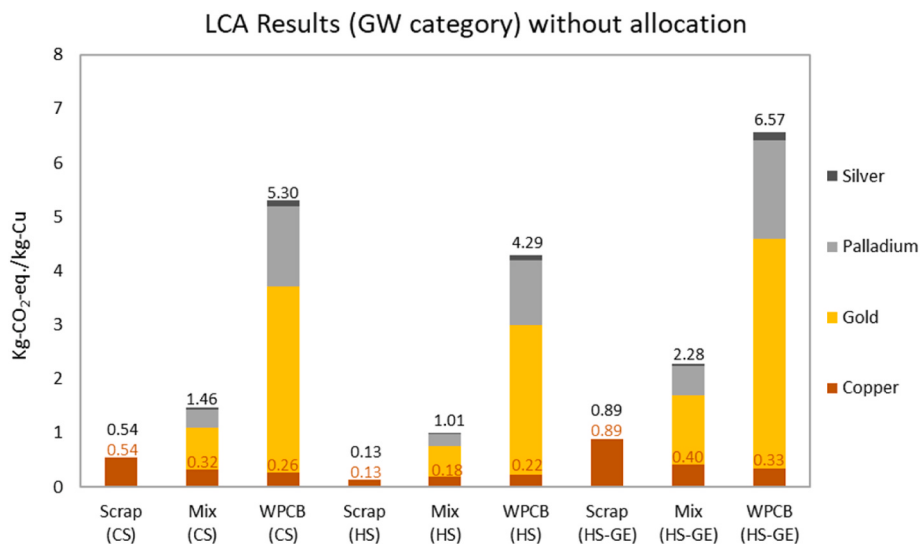


Fig. 4. Global warming LCA results without allocation. Brown numbers show copper values. CS: conventional scenario, HS: hydrogen scenario, HS-GE: hydrogen scenario with grid electricity. (For interpretation of the references to colour in this figure legend, the reader is referred to the Web version of this article.)

Table 5
LCA impact categories results (economic allocation). GE: grid electricity.

Ind.	Unit	Conventional Scenario			Hydrogen Scenario			Hydrogen Scenario (GE)		
		Scrap	Mix	WPCB	Scrap	Mix	WPCB	Scrap	Mix	WPCB
AD	kg Sb	5.0E-06	1.4E-06	6.4E-07	4.9E-06	1.1E-06	8.4E-07	5.7E-06	1.4E-06	9.6E-07
ADff	MJ	5.6E+00	1.4E+00	7.8E-01	1.5E+00	3.4E-01	2.6E-01	9.4E+00	2.7E+00	1.5E+00
Acid	kg SO ₂	1.9E-03	4.9E-04	2.0E-04	1.3E-03	2.6E-04	1.5E-04	2.7E-03	6.6E-04	3.6E-04
EU	kg PO ₄	1.5E-03	4.6E-04	2.3E-04	2.4E-04	5.7E-05	4.1E-05	4.2E-03	1.2E-03	6.5E-04
FWT	kg 1,4-DB	4.3E+01	2.2E+01	3.2E+00	4.7E+01	5.0E+00	4.2E+00	4.7E+01	5.2E+00	4.3E+00
GW	kg CO ₂	5.4E-01	3.2E-01	2.6E-01	1.3E-01	1.8E-01	2.2E-01	8.9E-01	4.0E-01	3.3E-01
HT	kg 1,4-DB	1.5E+01	1.5E+01	1.1E+01	1.2E+01	1.2E+01	1.2E+01	1.3E+01	1.2E+01	1.2E+01
MAT	kg 1,4-DB	3.1E+04	1.6E+05	1.5E+05	3.3E+04	1.3E+05	1.6E+05	3.5E+04	1.3E+05	1.6E+05
OLD	kg CFC-11	3.0E-08	7.1E-09	4.0E-09	1.4E-08	3.2E-09	2.6E-09	3.5E-08	9.4E-09	5.8E-09
PO	kg C ₂ H ₄	1.4E-04	3.6E-05	1.5E-05	5.9E-05	1.2E-05	7.3E-06	1.2E-04	2.9E-05	1.6E-05
TT	kg 1,4-DB	1.3E+00	3.9E-01	7.0E-02	1.4E+00	4.8E-01	1.2E-01	1.4E+00	4.8E-01	1.2E-01

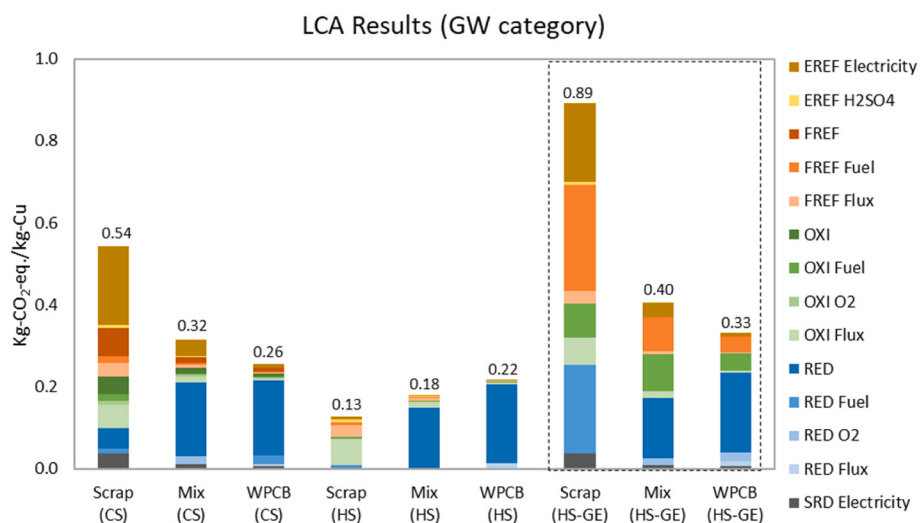


Fig. 5. Carbon footprint results disaggregated by steps (EREF: Electrorefining, FREF: Fire refining, OXI: Oxidation, RED: Reduction, SRD: Shredding). CS: conventional scenario, HS: hydrogen scenario, HS-GE: hydrogen scenario with grid electricity. (For interpretation of the references to colour in this figure legend, the reader is referred to the Web version of this article.)

addressed by adopting three feed cases and using thermodynamic, industrial, and experimental data in the studied simulation. Regarding hydrogen, its use in industry is viable (Torben and Steindor, 2023) and is gaining interest with ongoing projects (Hydrogen As the Reducing Agent). However, its implementation also present several limitations. Firstly, it requires renewable energies for its production, which require a significant amount of minerals. Secondly, transportation via pipeline requires a substantial investment or, in the case of in-situ production, an extensive area and favourable geographical conditions for renewable energy generation. Thirdly, the intermittency of renewable energies is an additional challenge requiring flexibility solutions (Scharf et al., 2024). However, the expected reduction of future green hydrogen cost could improve its economic viability (Frieden and Leker, 2024). Overall, this paper not only addresses the benefits of recycling copper, but further explores the potential of using renewable energies, essential for a more circular economy.

4. Conclusions

The present study demonstrated that the recovery of copper from WEEE have a 71–97 % lower carbon footprint compared to its primary extraction. The use of renewable energies (hydrogen and electricity) demonstrates the lowest carbon footprint (0.1–0.2 kg-CO₂-eq./kg-Cu), whereas the conventional scenario shows higher environmental impact (0.3–0.5 kg-CO₂-eq./kg-Cu). Thus, the circular economy goes beyond recycling by integrating renewable energies into the processes. However, the hydrogen scenario achieves the maximum carbon footprint reduction in the Scrap case (76% lower than conventional scenario) and a smaller reduction in the WPCB case (only 15%), due to the combustion of plastics present in WPCB. Therefore, separating plastics prior to smelting could provide a dual benefit for the industry, enabling the development of new products while reducing CO₂ emissions associated with plastics combustion.

Achieving low carbon footprint scenarios presents both challenges and opportunities for the industry. For instance, policies which promote design-for-recycling of PCB could reduce plastic content or enhance its separation. Additionally, securing a reliable supply of green hydrogen and renewable energy is crucial, as hydrogen production with non-renewable electricity results in a carbon footprint of 0.3–0.9 kg-CO₂-eq./kg-Cu, surpassing even conventional recycling. However, the transition from fossil fuel to renewable energy sources poses significant challenges including the variability, intermittency, and investment costs of these sources. Therefore, strategies and technologies, including grid modernization, energy storage, and demand response must be implemented to achieve the goals of energy transition.

CRediT authorship contribution statement

Jorge Torrubia: Writing – original draft, Visualization, Methodology, Data curation, Conceptualization. **Ashak Mahmud Parvez:** Writing – review & editing, Supervision, Methodology, Conceptualization. **Mohsin Sajjad:** Writing – review & editing, Validation, Methodology, Investigation, Conceptualization. **Felipe Alejandro García Paz:** Writing – original draft, Validation, Methodology, Data curation. **Karl Gerald van den Boogaart:** Writing – review & editing, Supervision, Software, Resources, Funding acquisition.

Declaration of competing interest

The authors declare that they have no known competing financial interests or personal relationships that could have appeared to influence the work reported in this paper.

Acknowledgements

This research was funded by Helmholtz Innovation Pool project EuK

(grant number: 1045129056). Moreover, the authors would like to thank KupferDigital project (grant number: 3145129008, funded by BMBF). Jorge Torrubia is grateful to project RESTORE funded by MICIU/AEI/10.13039/501100011033, and FEDER (EU) under grant agreement PID2023-148401OB-I00, and by MICIU/AEI/10.13039/501100011033, project REDOL funded by the European Union under Grant Agreement 101091668, and Fundación Bancaria Ibercaja for the IT 17 /22 Grant for international research stay.

Appendix A. Supplementary data

Supplementary data to this article can be found online at <https://doi.org/10.1016/j.jclepro.2024.144349>.

Data availability

Data will be made available on request.

References

- a. Enerdata renewable electricity production by country. <https://yearbook.enerdata.net/renewables/renewable-in-electricity-production-share.html>. (Accessed 1 October 2024).
- Anindya, A., 2012. Minor elements distribution during the smelting of WEEE with copper scrap. School of Civil, Environmental & Chemical Engineering Science, Engineering & Technology (SET) Portfolio RMIT University.
- b. Hydrogen as the reducing agent in the REcovery of metals and minerals from metallurgical waste. <https://cordis.europa.eu/project/id/958307>. (Accessed 24 April 2023).
- Bale, C.W., Bélisle, E., Chartand, P., Deckerov, S.A., Eriksson, G., Gheribi, A.E., Hack, K., Hung, I.H., Kang, Y.B., Melançon, J., et al., 2016. FactSage thermochemical software and database - 2010-2016. Calphad 54, 35–53.
- Banaszkiewicz, T., Chorowski, M., 2018. Energy consumption of air-separation adsorption methods. Entropy 20. <https://doi.org/10.3390/e20040232>.
- Chen, J., Wang, Z., Wu, Y., Li, L., Li, B., Pan, D., Zuo, T., 2019. Environmental benefits of secondary copper from primary copper based on life cycle assessment in China. Resour. Conserv. Recycl. 146, 35–44. <https://doi.org/10.1016/j.resconrec.2019.03.020>.
- Chen, M., Avarmaa, K., Taskinen, P., Klemettinen, L., Michallik, R., O'Brien, H., Jokilaakso, A., 2021. Handling trace elements in WEEE recycling through copper smelting—an experimental and thermodynamic study. Miner. Eng. 173. <https://doi.org/10.1016/j.mineeng.2021.107189>.
- Dong, D., van Oers, L., Tukker, A., van der Voet, E., 2020. Assessing the future environmental impacts of copper production in China: implications of the energy transition. J. Clean. Prod. 274. <https://doi.org/10.1016/j.jclepro.2020.122825>.
- Dong, D., Tukker, A., Steubing, B., van Oers, L., Rechberger, H., Alonso Aguilar-Hernandez, G., Li, H., Van der Voet, E., 2022. Assessing China's potential for reducing primary copper demand and associated environmental impacts in the context of energy transition and "zero waste" policies. Waste Manag. 144, 454–467. <https://doi.org/10.1016/j.wasman.2022.04.006>.
- European Commission: Joint Research Centre, Carrara, S., Alves Dias, P., Plazzotta, B., Pavel, C., 2020. Raw Materials Demand for Wind and Solar PV Technologies in the Transition towards a Decarbonised Energy System. Publications Office. ISBN 9789276162254.
- European Commission; Directorate-General for Internal Market; Industry; Entrepreneurship and SMEs, Grohol, M., Veeh, C., 2023. Study on the Critical Raw Materials for the EU 2023. Final Report.
- Felkl, L., Stelter, M., Charitos, A., 2023. Study of Metallothermic Reduction of Anode Furnace Slag Comparative Study on the Reduction of Copper Refining Slag by Metallic Reducing Agents.
- Forti, V., Baldé, C.P., Kuehr, R.E., 2018. Waste Statistics: Guidelines on Classification Reporting Adn Indicators, second ed. Bonn, Germany.
- Frieden, F., Leker, J., 2024. Future costs of hydrogen: a quantitative review. Sustain. Energy Fuels 8, 1806–1822.
- Fujita, T., Ono, H., Dodibba, G., Yamaguchi, K., 2014. Evaluation of a recycling process for printed circuit board by physical separation and heat treatment. Waste Manag. 34, 1264–1273. <https://doi.org/10.1016/j.wasman.2014.03.002>.
- Ghodrat, M., Rhamdhani, M.A., Brooks, G., Rashidi, M., Samali, B., 2017. A thermodynamic-based life cycle assessment of precious metal recycling out of waste printed circuit board through secondary copper smelting. Environ Dev 24, 36–49. <https://doi.org/10.1016/j.envdev.2017.07.001>.
- Ghodrat, M., Rhamdhani, M.A., Khaliq, A., Brooks, G., Samali, B., 2018. Thermodynamic analysis of metals recycling out of waste printed circuit board through secondary copper smelting. J. Mater. Cycles Waste Manag. 20, 386–401. <https://doi.org/10.1007/s10163-017-0590-8>.
- Ghodrat, M., Samali, B., Rhamdhani, M.A., Brooks, G., 2019. Thermodynamic-based exergy analysis of precious metal recovery out of waste printed circuit board through black copper smelting process. Energies 12. <https://doi.org/10.3390/en12071313>.

- Hong, J., Chen, Y., Liu, J., Ma, X., Qi, C., Ye, L., 2018. Life cycle assessment of copper production: a case study in China. *Int. J. Life Cycle Assess.* 23, 1814–1824. <https://doi.org/10.1007/s11367-017-1405-9>.
- Huisman, J., Leroy, P., Tertre, F., Ljunggren Söderman, M., Chancerel, P., Cassard, D., Løvik, A.N., Wäger, P., Kushnir, D., Susanne Rotter, V., et al., 2017. Prospecting Secondary Raw Materials in the Urban Mine and Mining Wastes (ProSUM). Final Report, Brussels, Belgium.
- Hund, K., Porta, D., La, Fabregas, T.P., Laing, T., Drexhage, J., 2020. Minerals for Climate Action: the Mineral Intensity of the Clean Energy Transition.
- Institute of scrap recycling Industries ISRI scrap specifications. <https://www.isrispecs.org/wp-content/uploads/2023/05/ISRI-Scrap-Specifications-Circular-updated-1.pdf>. (Accessed 1 February 2024).
- c International copper study group The World Copper Factbook Available online: <https://dev.icsg.org/wp-content/uploads/2021/11/ICSG-Factbook-2021.pdf>.
- Khalil, A., Rhamdhani, M.A., Brooks, G., Masood, S., 2014. Metal extraction processes for electronic waste and existing industrial routes: a review and Australian perspective. *Resources* 3, 152–179.
- Lazard, O., Youngs, R., 2021. The EU and Climate Security: toward Ecological Diplomacy.
- Mairizal, A.Q., Sembada, A.Y., Tse, K.M., Haque, N., Rhamdhani, M.A., 2023a. Carbon footprint assessment of waste PCB recycling through black copper smelting in Australia. In: Proceedings of the Proceedings of the 152nd TMS Annual Meeting & Exhibition (TMS 2023): "Energy Technology 2023, Carbon Dioxide Management and Other Technologies, pp. 107–118, 19-23 March 2023. San Diego.
- Mairizal, A.Q., Sembada, A.Y., Tse, K.M., Haque, N., Rhamdhani, M.A., 2023b. Assessment of mass and energy balance of waste printed circuit board recycling through hydrogen reduction in black copper smelting process. *Processes* 11. <https://doi.org/10.3390/pr11051506>.
- Mills, R., Copper: the most important metal we are running short of. <https://aheadoftherd.com/copper-the-most-important-metal-were-running-short-of-richard-mills/>. (Accessed 14 December 2022).
- National Minerals Information Center. Copper statistics and information. <https://www.usgs.gov/centers/national-minerals-information-center/copper-statistics-and-information>. (Accessed 14 December 2022).
- Nazari, A.M., Radzinski, R., Ghahreman, A., 2017. Review of arsenic metallurgy: treatment of arsenical minerals and the immobilization of arsenic. *Hydrometallurgy* 174, 258–281. <https://doi.org/10.1016/j.hydromet.2016.10.011>.
- Northey, S., Mohr, S., Mudd, G.M., Weng, Z., Giurco, D., 2014. Modelling future copper ore grade decline based on a detailed assessment of copper resources and mining. *Resour. Conserv. Recycl.* 83, 190–201. <https://doi.org/10.1016/j.resconrec.2013.10.005>.
- Outotec Research Center HSC Chemistry 10, Thermochemical and Process Simulation.
- Pokhrel, P., Lin, S.L., Tsai, C.T., 2020. Environmental and economic performance analysis of recycling waste printed circuit boards using life cycle assessment. *J. Environ. Manag.* 276. <https://doi.org/10.1016/j.jenvman.2020.111276>.
- Qu, G., Wei, Y., Li, B., Wang, H., Yang, Y., McLean, A., 2020. Distribution of copper and iron components with hydrogen reduction of copper slag. *J. Alloys Compd.* 824. <https://doi.org/10.1016/j.jallcom.2020.153910>.
- Röben, F.T.C., Schöne, N., Bau, U., Reuter, M.A., Dahmen, M., Bardow, A., 2021. Decarbonizing copper production by power-to-hydrogen: a techno-economic analysis. *J. Clean. Prod.* 306. <https://doi.org/10.1016/j.jclepro.2021.127191>.
- Sanjuan-Delmás, D., Alvarenga, R.A.F., Lindblom, M., Kampmann, T.C., van Oers, L., Guinée, J.B., Dewulf, J., 2022. Environmental assessment of copper production in Europe: an LCA case study from Sweden conducted using two conventional software-database setups. *Int. J. Life Cycle Assess.* 27, 255–266. <https://doi.org/10.1007/s11367-021-02018-5>.
- Scharf, H., Sauerbrey, O., Möst, D., 2024. What will Be the hydrogen and power demands of the process industry in a climate-neutral Germany? *J. Clean. Prod.* 466. <https://doi.org/10.1016/j.jclepro.2024.142354>.
- Schlesinger, M.E., King, M.J., Sole, K.C., Davenport, W.G., Alvear Flores, G.R.F., 2021. Extractive Metallurgy of Copper, sixth ed. 6th ed.
- Shiva Kumar, S., Himabindu, V., 2019. Hydrogen production by PEM water electrolysis – a review. *Mater Sci Energy Technol* 2, 442–454.
- Shuva, M.A.H., Rhamdhani, M.A., Brooks, G.A., Masood, S., Reuter, M.A., 2016. Thermodynamics data of valuable elements relevant to E-waste processing through primary and secondary copper production: a review. *J. Clean. Prod.* 131, 795–809.
- d. Sicon EcoShred catalog available online. <https://sicontechnology.com/wp-content/uploads/ecoshred-vertex-e.pdf>. (Accessed 14 December 2022).
- Tabelin, C.B., Park, I., Phengsaart, T., Jeon, S., Villacorte-Tabelin, M., Alonso, D., Yoo, K., Ito, M., Hiroyoshi, N., 2021. Copper and critical metals production from porphyry ores and E-wastes: a review of resource availability, processing/recycling challenges, socio-environmental aspects, and sustainability issues. *Resour. Conserv. Recycl.* 170. <https://doi.org/10.1016/j.resconrec.2021.105610>.
- Torben, Edens, Steindor, J., 2023. Using hydrogen as a reductant in fire refining at Aurubis hamburg's "Down-Town" smelter. In: Proceedings of the Proceedings of the 61st Conference of Metallurgists, COM 2022. Springer International Publishing, Cham, pp. 211–228.
- Torrubia, J., Valero, A., Valero, A., 2022. Thermodynamic rarity assessment of mobile phone PCBs: a physical criticality indicator in times of shortage. *Entropy* 24. <https://doi.org/10.3390/e24010100>.
- Torrubia, J., Valero, A., Valero, A., 2023a. Energy and carbon footprint of metals through physical allocation. Implications for energy transition. *Resour. Conserv. Recycl.* 199, 107281. <https://doi.org/10.1016/j.resconrec.2023.107281>.
- Torrubia, J., Valero, A., Valero, A., Lejuez, A., 2023b. Challenges and opportunities for the recovery of critical raw materials from electronic waste: the Spanish perspective. *Sustainability* 15, 1393. <https://doi.org/10.3390/su15021393>.
- e. Trading economics price of metals and natural gas. <https://tradingeconomics.com/commodities>. (Accessed 14 December 2022).
- Valero Navazo, J.M., Villalba Méndez, G., Talens Peiró, L., 2014. Material flow analysis and energy requirements of mobile phone material recovery processes. *Int. J. Life Cycle Assess.* 19, 567–579. <https://doi.org/10.1007/s11367-013-0653-6>.
- Van der Voet, E., Van Oers, L., Verboon, M., Kuipers, K., 2019. Environmental implications of future demand scenarios for metals: methodology and application to the case of seven major metals. *J. Ind. Ecol.* 23, 141–155. <https://doi.org/10.1111/jiec.12722>.
- Zhang, W., Li, Z., Dong, S., Qian, P., Ye, S., Hu, S., Xia, B., Wang, C., 2021. Analyzing the environmental impact of copper-based mixed waste recycling—a LCA case study in China. *J. Clean. Prod.* 284. <https://doi.org/10.1016/j.jclepro.2020.125256>.
- Zhang, J., Tian, X., Chen, W., Geng, Y., Wilson, J., 2022. Measuring environmental impacts from primary and secondary copper production under the upgraded technologies in key Chinese enterprises. *Environ. Impact Assess. Rev.* 96. <https://doi.org/10.1016/j.eiar.2022.106855>.